AIP | The Journal of Chemical Physics

# Communication: Intraparticle segregation of structurally homogeneous polyelectrolyte microgels caused by long-range Coulomb repulsion

Artem M. Rumyantsev, Andrey A. Rudov, and Igor I. Potemkin

Citation: The Journal of Chemical Physics **142**, 171105 (2015); doi: 10.1063/1.4919951
View online: http://dx.doi.org/10.1063/1.4919951
View Table of Contents: http://scitation.aip.org/content/aip/journal/jcp/142/17?ver=pdfcov
Published by the AIP Publishing

**Articles you may be interested in**

Modeling the effects of pH and ionic strength on swelling of polyelectrolyte gels
J. Chem. Phys. **142**, 114904 (2015); 10.1063/1.4914924

Theory of volume transition in polyelectrolyte gels with charge regularization
J. Chem. Phys. **136**, 134901 (2012); 10.1063/1.3698168

Effect of the concentration on sol–gel transition of telechelic polyelectrolytes
J. Chem. Phys. **134**, 034903 (2011); 10.1063/1.3532090

Long-range many-body polyelectrolyte bridging interactions
J. Chem. Phys. **122**, 204902 (2005); 10.1063/1.1908870

Swelling of polyelectrolyte networks
J. Chem. Phys. **122**, 154903 (2005); 10.1063/1.1882275

How can you **REACH 100%** of researchers at the Top 100 Physical Sciences Universities? (TIMES HIGHER EDUCATION RANKINGS, 2014)
With *The Journal of Chemical Physics*.

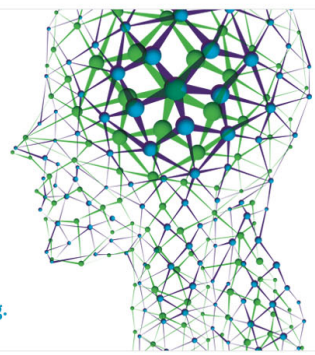

AIP | The Journal of Chemical Physics
THERE'S POWER IN NUMBERS. Reach the world with AIP Publishing.

This article is copyrighted as indicated in the article. Reuse of AIP content is subject to the terms at: http://scitation.aip.org/termsconditions. Downloaded to IP: 134.61.147.93 On: Thu, 07 May 2015 13:55:08

# Communication: Intraparticle segregation of structurally homogeneous polyelectrolyte microgels caused by long-range Coulomb repulsion

Artem M. Rumyantsev, Andrey A. Rudov, and Igor I. Potemkin[a)]
*Physics Department, Lomonosov Moscow State University, Moscow 119991, Russia and DWI—Leibniz-Institut für Interaktive Materialien, Aachen 52056, Germany*

(Received 1 April 2015; accepted 28 April 2015; published online 7 May 2015)

Structurally homogeneous polyelectrolyte microgels in dilute aqueous solutions are shown to exhibit inhomogeneous density profile including intraparticle "phase" coexistence of hollow core and dense "skin." This effect is a consequence of long-range Coulomb repulsion of charged groups which appear because of entropy-driven escape of monovalent counterions into the outer solvent. Excess of the charged groups at the periphery of the microgel particle reduces electrostatic energy and overall free energy of the system despite a penalty in the elastic free energy of strongly stretched subchains in the hole. This finding can serve as additional tool controlling encapsulation, transport, and release of high- and low-molecular-weight species in processes where the microgels are used as delivery systems. © *2015 AIP Publishing LLC.* [http://dx.doi.org/10.1063/1.4919951]

Internal structure of polyelectrolyte microgels (μGs) resembles elements of macroscopic polymer network: linear charged chains (subchains) are covalently linked with each other into three-dimensional frame of the size in the range between tens of nanometers and few microns.[1] In contrast to macroscopic polyelectrolyte gels, electric neutrality of the μGs in aqueous dilute solutions is violated due to partial escape of monovalent counterions into the outer solvent caused by their thermal motion. In other words, the electrostatic energy is too weak to fully overcome an entropic tendency of the counterions to occupy as larger volume of the system as possible. As a result, the μGs are highly swollen in a good solvent due to both long-range repulsion of unscreened charged monomer units and exerting osmotic pressure of mobile counterions which are trapped inside the μG.[2–4] Also their colloidal stability in a good solvent is enhanced because of long-range electrostatic repulsion between the particles.

Up to now, the existing theories treat the μGs as homogeneously charged, penetrable, and elastic spherical objects.[5–8] Counterion distribution is usually calculated with the Poisson-Boltzmann approach which exploits the homogeneous charged distribution inside the microgel.[5–9] On the other hand, similarly to the macroscopic gels,[10] the μGs exhibit different properties at different length scales. Liquid-like behavior is characteristic at the length-scales smaller than the mesh-size, where each subchain does not feel connectivity into the network. Elastic, solid-like response is revealed at the length scales larger than the mesh-size.[10] Combination of the long-range Coulomb repulsion between charged groups together with ability of monomer units to "flow" at the small length scales can be responsible for unusual behavior.

In the present paper, we propose a mean-field theory and computer simulations which predict equilibrium a center-to-periphery mass redistribution with formation of a hollow structure of strongly stretched subchains in the center of the μG and dense "skin" at the periphery. This effect is a consequence of a competition between long-range repulsion of unscreened charged monomer units tending to bring them to the periphery of the particle and elasticity of the subchains preventing long-distance migration of the charges. Repulsive or attractive short-range interactions between monomer units, which are determined by the solvent quality, can both promote and suppress the effect.

The electrostatics driven center-to-periphery migration can easily be explained on the basis of elementary physics via comparison of the electrostatic energies of two spheres of the radius $R$ having different distributions of the charge $Q$. The sphere with the surface charge has lower energy than the sphere with homogeneously distributed volume charge, $Q^2/2R < 3Q^2/5R$. Therefore, migration of the charge from the volume to the surface is accompanied by the decrease of the electrostatic energy. This effect should be universal for many charged and intrinsically soft systems as soon as local electric neutrality is violated. It is unusual that the intraparticle "phase" coexistence is caused by the long-range Coulomb repulsion and elasticity of the subchains rather than short-range attraction of monomer units which is typical for many polymer systems.[11–14]

The microgel is considered as a set of $\nu$ elastically active, flexible subchains, each of $N$ segments. The fraction of charged monovalent units $f$ is assumed to be very small, $f << 1$. In order to prove the concept of intraparticle segregation, let us consider first the so-called Pincus regime[15] when all monovalent counterions leave the particle into the outer solvent and can be neglected in the theoretical approach. Such regime is realized under strong (infinite) dilution of the system. The free energy of the single μG comprises electrostatic, elastic, and conventional Flory-Huggins contributions,

a)Author to whom correspondence should be addressed. Electronic mail: igor@polly.phys.msu.ru

 © 2015 AIP Publishing LLC

This article is copyrighted as indicated in the article. Reuse of AIP content is subject to the terms at: http://scitation.aip.org/termsconditions. Downloaded to IP: 134.61.147.93 On: Thu, 07 May 2015 13:55:08

$$\frac{F_{total}}{k_BT} = \frac{l_B}{2}\int d^3r \int d^3r' \frac{\rho(r)\rho(r')}{|\mathbf{r}-\mathbf{r}'|} + \int_0^R dr r^2 4\pi F(\phi(r)) + \mu\left(\int_0^R dr r^2 4\pi\phi(r) - N\nu a^3\right). \quad (1)$$

Here, $l_B = e^2/(k_BT\varepsilon)$ is the Bjerrum length, $e$ and $\varepsilon$ are the elementary charge and dielectric constant of the solvent, respectively, and $k_BT$ is the thermal energy. Concentration of the charged groups in the μG $\rho(r)$ is proportional to the polymer volume fraction $\phi(r)$, $\rho(r) = f\phi(r)/a^3$, which is assumed to have a spherical symmetry; $r$ is the radial coordinate, $0 \le r \le R$; $a$ is the segment length. The Lagrange multiplier $\mu$ introduces normalization of the function $\phi$ (space-filling condition).[16] In Eq. (1), $F = F_{FH} + F_{el}$, and conventional Flory-Huggins term describes solvent entropy and short-range interactions between the monomer units, $F_{FH}a^3 = (1-\phi(r))\ln(1-\phi(r)) - \chi\phi^2(r)$; $\chi$ is dimensionless interaction parameter. The elastic contribution $F_{el}$ is responsible for the entropic losses of the subchains under their stretching or collapse with respect to the Gaussian size. The losses in the collapsed state can be estimated as $3Na^2/2L^2$ per subchain, where $L$ is the end-to-end distance of the subchain.[17] It can be rewritten in terms of the polymer volume fraction (continuous limit) as $3(\phi(r)/\phi_0)^{2/3}/2$, where $\phi_0 = 6/\pi\sqrt{N}$ is the polymer volume fraction of Gaussian subchains (reference state). The number of the subchains per unit volume can be calculated as $\phi(r)/Na^3$. It is known that the end-to-end distance of the subchain in a polyelectrolyte microgel is proportional to its contour length $L \sim N$ both for the Pincus and osmotic regimes.[2] Therefore, the Flory approach for the description of the subchain stretching (the elastic free energy $\sim 3L^2/2Na^2$) is doubtful because it can result in the stretching exceeding the contour length. To overcome this problem, we use a non-linear dependence of the end-to-end distance on the applied force $p$,[18–20] $L = aN(\coth(\beta) - 1/\beta)$, $\beta = ap/k_BT$. This dependence reproduces the Hook's law at small stretching forces, $\beta \ll 1$, and the full stretching limit can be attained at infinite force only. Then, the elastic contribution to the free energy is calculated as an action of the applied force $p$: $\int \beta(L)dL/a = \beta L/a - \int L(\beta)d\beta/a$. The final expression for the elastic free energy per unit volume takes the form[18–20]

$$F_{el} = \frac{\phi(r)}{Na^3}\left(\frac{3}{2}\left(\frac{\phi(r)}{\phi_0}\right)^{2/3} + N\left(\beta(r)\coth\beta(r) - \ln\frac{\sinh\beta(r)}{\beta(r)} - 1\right)\right),$$
$$\coth\beta(r) - \frac{1}{\beta(r)} = \frac{1}{\sqrt{N}}\left(\frac{\phi_0}{\phi(r)}\right)^{1/3}, \quad (2)$$

which depends on $\phi(r)$ implicitly. The equilibrium distribution of the polymer inside the μG is calculated via minimization of the total free energy, Eq. (1), with respect to the volume fraction $\phi(r)$, multiplier $\mu$, and to the radius of the microgel $R$. The result can be reduced to the following set of equations:

$$\begin{cases} \dfrac{d}{dr}\left(r^2\dfrac{d\phi}{dr}\dfrac{d^2F}{d\phi^2}\right) = \dfrac{4\pi l_B f^2}{a^3}\phi r^2 \\ F - \phi\dfrac{dF}{d\phi}\Big|_{r=R} = 0, \quad \dfrac{d\phi}{dr}\dfrac{d^2F}{d\phi^2}\Big|_{r=R} = \dfrac{l_B f^2 N\nu}{R^2} \\ \displaystyle\int_0^R dr r^2 4\pi\phi = N\nu a^3 \end{cases}. \quad (3)$$

To analyze effects of the solvent quality and the fraction of charged groups on the μG structure, we have fixed the parameters $l_B/a = 1$, $\nu = 1000$, and $N = 25$ and solved Eq. (3) numerically at different values of $\chi$ and $f$. Fig. 1 depicts that increasing fraction of charged groups inside the microgel placed into a poor solvent, $\chi = 1$, induces inhomogeneous swelling. If the μG is uncharged, $f = 0$, the polymer density is constant. Gradual increase of $f$ first leads to continuous increase of the density at the periphery ($f = 0.01$). Further increase of $f$, $f = 0.015$-$0.05$, makes the profile discontinuous: nearly constant, very low polymer volume fraction is characteristic for the central part of the μG, and the periphery is ca 100 times denser. Therefore, the subchains of the inner, hollow part of the microgel are practically fully stretched and the subchains at the periphery are collapsed. Such intraparticle "phase" coexistence is controlled by the fraction of charged groups: the hole expands while the shell narrows upon charging the μG, Fig. 1. Despite of the penalties in the elastic free energy and the surface energy of inner interface, the system gains in the electrostatic energy because a high fraction of charged groups is localized at the periphery due to their mobility at finite distances. Effect of the solvent quality is demonstrated in Fig. 2. In a very bad solvent, $\chi = 2$, Fig. 2(a), the effective short-range attraction between insoluble monomer units dominates over the Coulomb repulsion and the density profile is practically constant. Improvement of the solvent quality first leads to continuous mass redistribution to the periphery which is followed by the hole formation and its growth with the decrease of $\chi$, Fig. 2(a). However, this growth stops at a certain value of $\chi$ and the size of the hole diminishes with the decrease of $\chi$ in a good solvent regime ($\chi < 0.5$, Fig. 2(b)). The hole disappears at $\chi \approx 0.3$, where the density profile becomes continuous, Fig. 2(b). Such behavior is related to the short-range repulsion between monomer units in a good

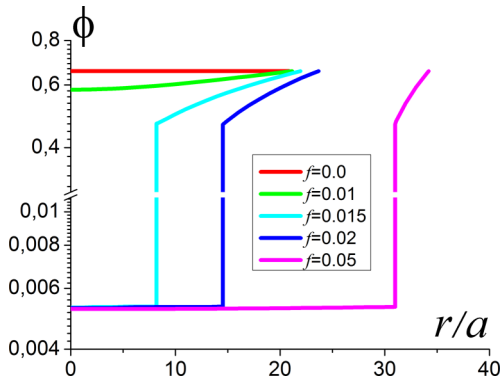


FIG. 1. Polymer volume fraction of the microgel $\phi$ as a function of radial coordinate $r$ at fixed value of the interaction parameter $\chi = 1$ and different values of the fraction of charged groups. The curves end at $r = R$.

This article is copyrighted as indicated in the article. Reuse of AIP content is subject to the terms at: http://scitation.aip.org/termsconditions. Downloaded to IP: 134.61.147.93 On: Thu, 07 May 2015 13:55:08

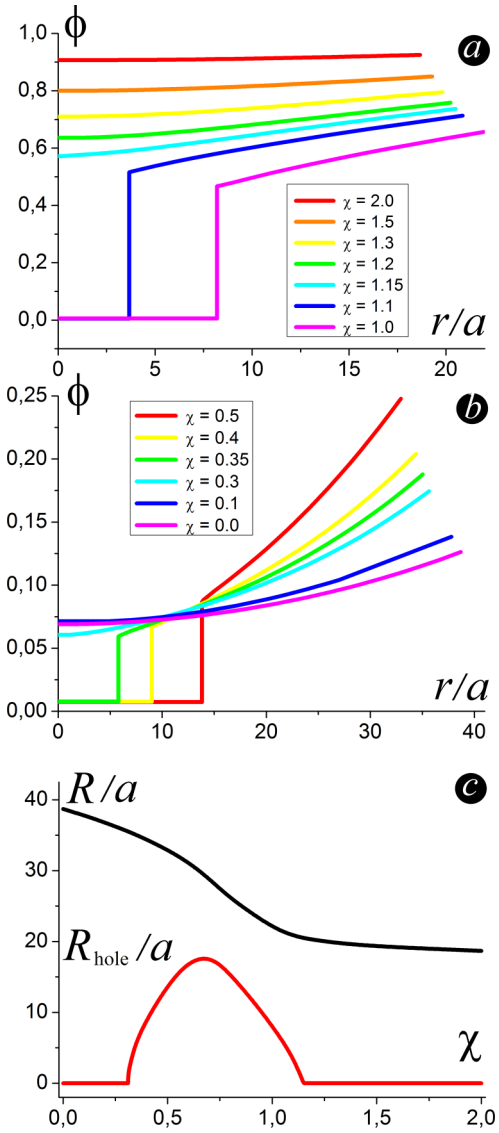


FIG. 2. Polymer volume fraction $\phi$ as a function of radial coordinate $r$ at fixed value of the fraction of charged groups, $f = 0.015$, and different values of the interaction parameter $\chi$: poor solvent from $\chi = 1$ to 2 (a) and good solvent from $\chi = 0$ to 0.5 (b). Radius of the microgel, $R$, and of the hole, $R_{\text{hole}}$, versus interaction parameter $\chi$ (c).

solvent which increases distance between charged groups and promotes gain in the electrostatic energy even without distinct shell formation. Conditions for the hole formation are clearly summarized in Fig. 2(c): the microgel is essentially hollow around the theta-point ($\chi = 1/2$).

Effect of counterion localization inside the μG at finite concentration of the particles or at higher fraction of charged units in the subchains does not change the aforementioned predictions of the intraparticle segregation. The counterions can be taken into account, if we introduce the ideal gas term into the integral of Eq. (1), $n(r)\ln(n(r)a^3/e)$, and modify the reduced charge density in the first term of Eq. (1) as $\rho(r)a^3 = f\phi(r) - n(r)$ at $0 < r < R$ and $\rho(r)a^3 = -n(r)$ at $R < r < R_{\text{out}}$. Here, $R_{\text{out}}$ is the radius of the solution elementary cell which is approximated by a sphere (i.e., the volume of the system per one μG). Taking into account a macroscopic electric neutrality of the system $\int_0^{R_{out}} dr 4\pi r^2 \rho(r) = 0$ via the second Lagrange multiplier, the total free energy is calculated by minimization with respect to the functions $\phi(r)$, $n(r)$ and radius $R$ at fixed value of the parameter $R_{\text{out}}$ which quantifies concentration of the μG particles.

The polymer volume fraction of the μG in the presence of counterions is shown in Fig. 3(a). The intraparticle segregation is not preserved by the counterions. Furthermore, the difference in the densities of the hole and the skin increases as compared to the Pincus regime ($R_{\text{out}} = 2500$ and $R_{\text{out}} = \infty$, respectively). This effect is related to partial screening of the electrostatic repulsion of monomer units in the skin by the counterions whose concentration has local maximum there (Fig. 3(b), $R_{\text{out}} = 2500$). Further concentrating the μG solution, $R_{\text{out}} = 250$, increases concentration of counterions inside the microgel, Fig. 3(b), which weakens the electrostatic repulsion and makes the density profile continuous, Fig. 3(a).

The mean-field calculations are supported by computer simulations. We performed molecular dynamics simulations of a single polyelectrolyte microgel within a coarse-grained model and implicit solvent. The microgel is designed as follows. Fully stretched subchains of an ideal microgel (all subchains have equal length) are connected through tetrafunctional cross-links[21] and repeat a unit cell of the diamond crystal lattice. Then, we construct a cubic frame consisting of $6 \times 6 \times 6$ unit cells. To provide a "spherical" shape of the microgel, we inscribe a sphere into the cubic frame and "crop" all monomer units which are outside the sphere. As a result,

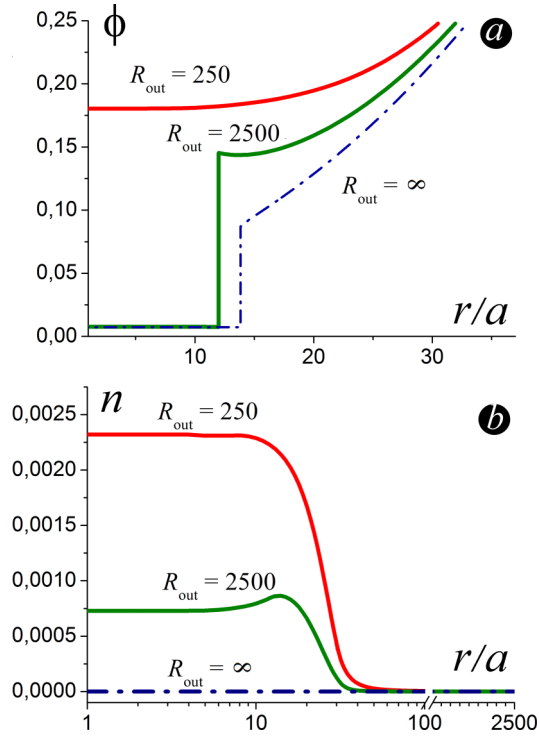


FIG. 3. Polymer $\phi$ (a) and counterion $n$ (b) volume fractions as functions of the radial coordinate $r$ at different values of the volume per μG (radius $R_{\text{out}}$) and fixed value of the fraction of charged groups, $f = 0.015$. Dotted lines correspond to the regime of infinite dilution of the solution (Pincus regime). The solvent quality corresponds to the theta conditions, $\chi = 1/2$.

This article is copyrighted as indicated in the article. Reuse of AIP content is subject to the terms at: http://scitation.aip.org/termsconditions. Downloaded to IP: 134.61.147.93 On: Thu, 07 May 2015 13:55:08

we obtain a microgel containing both subchains and dangling chains. To avoid dependence of final results on the choice of the particular structure, the center of the sphere was taken to coincide with the center of the cell, with a cross-link and few other intermediate positions. In addition to the thermodynamic averaging, the final results (density profiles) were averaged over the ensemble of the different μGs. Each subchain consists of $N = 15$ particles (beads); the average number of the beads (including cross-linkers) in the microgel is $N_{\text{total}} = 5990$. Charged monomer units are randomly (homogeneously) distributed throughout the microgel; their fraction was fixed, $f = 0.1$. Counterions provide overall electric neutrality of the system. Both charged and uncharged monomer units of the μG and counterions are modeled as Lennard-Jones particles (beads) of the diameter $\sigma$ and the same mass $m$. The interaction between any pair of the particles is described through the truncated-shifted Lennard-Jones potential.[22,23] Similarly to the model described in Ref. 22, we set the cutoff distance $r_{\text{cut}} = 2.5\sigma$ for intermonomer interactions and $r_{\text{cut}} = 2^{1/6}\sigma$ for all other pairwise interactions. The solvent quality is quantified by the Lennard-Jones intermonomer interaction parameter $\varepsilon_{LJ}$ which is varied between 0.01 (good solvent) and 1 $k_{\text{B}}T$ (poor solvent). The value of the Lennard-Jones parameter for monomer-counterion and counterion-counterion interactions was set to 1 $k_{\text{B}}T$.[23,24] Electrostatic interactions between any pair of charged particles are described by Coulomb potential. The value of the Bjerrum length was fixed and equal to $l_{\text{B}} = 3\sigma$, which corresponds to aqueous solutions. Connectivity of the particles into polymer chains was realized by the finite extension nonlinear elastic (FENE) potential (see Ref. 23 for details). The simulations were performed using the open source software LAMMPS.[25] The simulation cell was a cubic box of the size $L_x = L_y = L_z = 250\sigma$. The calculations were carried out in NVT ensemble with periodic boundary conditions. The electrostatic interactions between charged particles of the system were calculated by the Ewald summation method with the accuracy of $10^{-5}$. Annealing of the microgel at various values of the interaction parameter $\varepsilon_{LJ}$ was performed during $20 \times 10^6$ simulation steps. The averaging has been made in the last $5 \times 10^6$ steps.

The polymer volume fraction profiles are shown in Fig. 4. Initial weakly inhomogeneous monomer density distribution in very good solvent, Fig. 4(a), reveals essential instability and mass redistribution towards the periphery under approximately theta-conditions (peak in Fig. 4(b)). Then, the peak grows further with $\varepsilon_{LJ}$ which manifests that the collapse of the μG is accompanied by formation of the distinct hole in the center and the dense skin at the periphery, Figs. 4(d) and 4(e). Such behavior corresponds to the mean-field results, Fig. 2: the poorer the solvent, the higher the concentration jump. Formation of the hollow structure and nanophase segregation under poor solvent conditions was also predicted recently with Monte Carlo simulations.[14] However, the authors did not propose explanation of the effect.

In conclusion, we have demonstrated using a mean-field approach and molecular dynamics simulations that structurally homogeneous polyelectrolyte microgels in dilute aqueous solutions can have inhomogeneous density distribution including intraparticle "phase" coexistence: the hole of strongly stretched subchains in the center of the particle and the dense skin at the periphery. The found effect gives a straightforward way for controlled encapsulation, transport, and release of high- and low-molecular-weight species in many processes

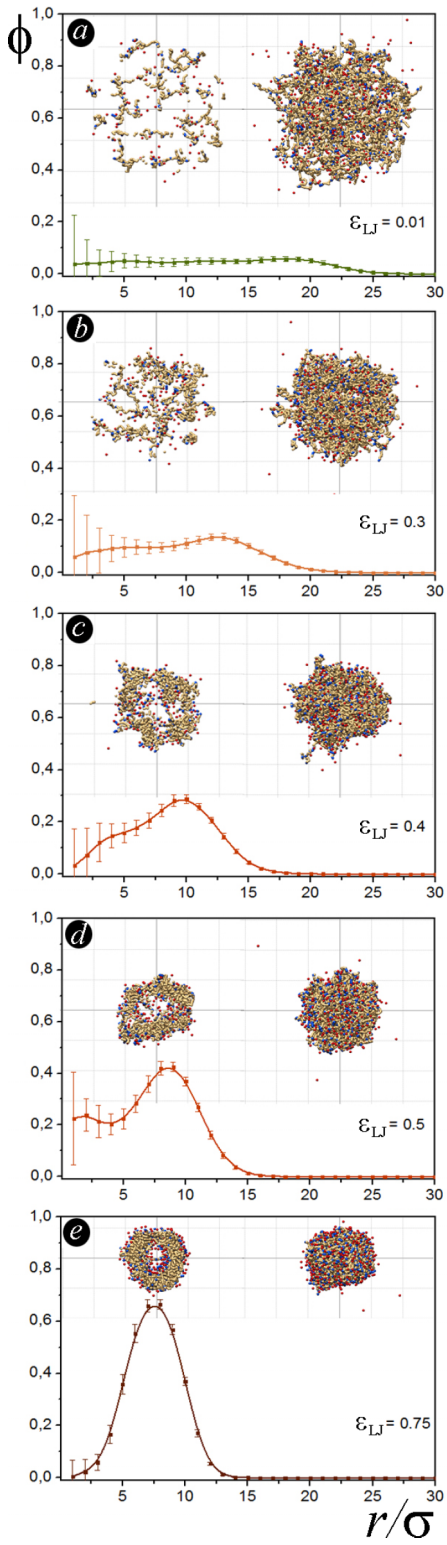


FIG. 4. Polymer volume fraction $\phi$ of polyelectrolyte microgel as a function of radial coordinate $r$ at different values of the Lennard-Jones interaction parameter $\varepsilon_{LJ}$: 0.01 (a), 0.3 (b), 0.4 (c), 0.5 (d), 0.75 $k_{\text{B}}T$ (e). The fraction of charged groups is fixed, $f = 0.1$. Left and right snapshots in each figure correspond to cross section through the center of mass and side-view of the microgel, respectively.

This article is copyrighted as indicated in the article. Reuse of AIP content is subject to the terms at: http://scitation.aip.org/termsconditions. Downloaded to IP: 134.61.147.93 On: Thu, 07 May 2015 13:55:08

where the μGs serve as delivery systems. For example, pH-sensitive microgels based on *N*-vinylcaprolactam with ionizable itaconic acid or vinylimidazole groups[1] can be loaded by some species in neutral state (the microgel surface is penetrable) and can be transportable in the charged state when the shell of the μG prohibits release of the loaded species.

Financial support of the German Science Foundation (DFG) within the SFB 985 "Functional Microgels and Microgel Systems" and Russian Foundation for Basic Research is gratefully acknowledged. The simulations were performed on multiteraflop supercomputer Lomonosov at Moscow State University.

[1]W. Richtering and A. Pich, Soft Matter **8**, 11423–11430 (2012).
[2]E. Yu. Kramarenko, A. R. Khokhlov, and K. Yoshikawa, Macromolecules **30**, 3383–3388 (1997).
[3]I. I. Potemkin, V. V. Vasilevskaya, and A. R. Khokhlov, J. Chem. Phys. **111**, 2809–2817 (1999).
[4]I. I. Potemkin, S. A. Andreenko, and A. R. Khokhlov, J. Chem. Phys. **115**, 4862–4872 (2001).
[5]F. T. Wall and J. Berkowitz, J. Chem. Phys. **26**, 114–122 (1957).
[6]G. C. Claudio, K. Kremer, and C. Holm, J. Chem. Phys. **131**, 094903 (2009).
[7]P. K. Jha, J. W. Zwanikken, J. J. de Pablo, and M. O. de la Cruz, Curr. Opin. Solid State Mater. Sci. **15**, 271–276 (2011).
[8]A. R. Denton, Phys. Rev. E **67**, 011804 (2003).
[9]A. Chepelianskii, F. Mohammad-Rafiee, E. Trizac, and E. Raphaël, J. Phys. Chem. B **113**, 3743–3749 (2009).
[10]S. V. Panyukov and I. I. Potemkin, J. Phys. I **7**, 273–289 (1997).
[11]K. B. Zeldovich, E. E. Dormidontova, A. R. Khokhlov, and T. A. Vilgis, J. Phys. II **7**, 627–635 (1997).
[12]A. V. Dobrynin, M. Rubinstein, and S. P. Obukhov, Macromolecules **29**, 2974–2979 (1996).
[13]K. A. Wu, P. K. Jha, and M. Olvera de la Cruz, Macromolecules **45**, 6652–6657 (2012).
[14]M. Quesada-Perez and A. Martin-Molina, Soft Matter **9**, 7086–7094 (2013).
[15]P. Pincus, Macromolecules **24**, 2912–2919 (1991).
[16]I. I. Potemkin, Eur. Phys. J. E **12**, 207–210 (2003).
[17]A. Yu. Grosberg and A. R. Khokhlov, *Statistical Physics of Macromolecules* (American Institute of Physics, New York, 1994).
[18]W. Kuhn and F. Grün, Kolloid-Z. **101**, 248–271 (1942).
[19]S. S. Sheiko, S. A. Prokhorova, K. L. Beers, K. Matyjaszewski, I. I. Potemkin, A. R. Khokhlov, and M. Möller, Macromolecules **34**, 8354–8360 (2001).
[20]I. I. Potemkin and K. I. Popov, J. Chem. Phys. **129**, 124901 (2008).
[21]H. Kobayashi and R. G. Winkler, Polymers **6**, 1602–1617 (2014).
[22]S. Toxvaerd and J. C. Dyre, J. Chem. Phys. **134**, 081102 (2011).
[23]M. A. Pigaleva, I. V. Portnov, A. A. Rudov, I. V. Blagodatskikh, T. E. Grigoriev, M. O. Gallyamov, and I. I. Potemkin, Macromolecules **47**, 5749–5758 (2014).
[24]J. Jeon and A. V. Dobrynin, Macromolecules **40**, 7695–7706 (2007).
[25]S. Plimpton, J. Comput. Phys. **117**, 1–19 (1995).

This article is copyrighted as indicated in the article. Reuse of AIP content is subject to the terms at: http://scitation.aip.org/termsconditions. Downloaded to IP: 134.61.147.93 On: Thu, 07 May 2015 13:55:08